

# A key role for G-CSF–induced neutrophil production and trafficking during inflammatory arthritis

Jo L. Eyles,<sup>1,2</sup> Michael J. Hickey,<sup>3</sup> M. Ursula Norman,<sup>3</sup> Ben A. Croker,<sup>1</sup> Andrew W. Roberts,<sup>1</sup> Sarah F. Drake,<sup>1</sup> Will G. James,<sup>3</sup> Donald Metcalf,<sup>1</sup> Ian K. Campbell,<sup>1</sup> and Ian P. Wicks<sup>1</sup>

<sup>1</sup>The Walter and Eliza Hall Institute of Medical Research, Parkville; <sup>2</sup>University of Melbourne, Parkville; and <sup>3</sup>Centre for Inflammatory Diseases, Monash University, Victoria, Australia

**We have previously shown that G-CSF–deficient (G-CSF<sup>-/-</sup>) mice are markedly protected from collagen-induced arthritis (CIA), which is the major murine model of rheumatoid arthritis, and now investigate the mechanisms by which G-CSF can promote inflammatory disease. Serum G-CSF levels were significantly elevated during CIA. Reciprocal bone marrow chimeras using G-CSF<sup>-/-</sup>, G-CSFR<sup>-/-</sup>, and wild-type (WT) mice identified nonhematopoietic cells as the major producers of G-CSF and hematopoietic cells as the**

**major responders to G-CSF during CIA. Protection against CIA was associated with relative neutropenia. Depletion of neutrophils or blockade of the neutrophil adhesion molecule, Mac-1, dramatically attenuated the progression of established CIA in WT mice. Intravital microscopy of the microcirculation showed that both local and systemic administration of G-CSF significantly increased leukocyte trafficking into tissues in vivo. G-CSF–induced trafficking was Mac-1 dependent, and G-CSF up-regulated CD11b ex-**

**pression on neutrophils. Multiphoton microscopy of synovial vessels in the knee joint during CIA revealed significantly fewer adherent Gr-1<sup>+</sup> neutrophils in G-CSF<sup>-/-</sup> mice compared with WT mice. These data confirm a central proinflammatory role for G-CSF in the pathogenesis of inflammatory arthritis, which may be due to the promotion of neutrophil trafficking into inflamed joints, in addition to G-CSF–induced neutrophil production. (Blood. 2008;112:5193-5201)**

## Introduction

G-CSF is used clinically to treat chemotherapy-associated neutropenia and to mobilize hematopoietic stem cells for transplantation. G-CSF therapy is generally well tolerated by patients and donors in these clinical settings, however numerous reports link G-CSF administration with vascular complications and exacerbation of underlying inflammatory conditions, including Felty syndrome and rheumatoid arthritis (RA).<sup>1-9</sup> Elevated levels of G-CSF have been reported in serum and synovial fluid of RA patients, and correlated with disease activity and severity.<sup>10</sup> G-CSF administration exacerbates collagen-induced arthritis (CIA) in mice<sup>11</sup> and also a passive-transfer model of CIA in rats.<sup>12</sup> We have previously reported that mice deficient in G-CSF (G-CSF<sup>-/-</sup> mice) are profoundly resistant to CIA, and that administration of neutralizing anti-G-CSF antibodies to WT mice after the onset of CIA prevents disease progression.<sup>13</sup> Protection of G-CSF<sup>-/-</sup> mice in CIA was associated with reduced neutrophil production,<sup>13</sup> but these studies did not address whether G-CSF itself may have other proinflammatory effects.

Administered G-CSF increases peripheral blood neutrophil numbers,<sup>14</sup> and endogenous G-CSF is important for basal granulopoiesis, as demonstrated by relative neutropenia in mice deficient in G-CSF or the G-CSF receptor (G-CSFR).<sup>15,16</sup> Infiltration of target tissues by neutrophils is characteristic of many inflammatory conditions, and neutrophils are a major leukocyte population found within inflamed joints in RA and CIA.<sup>17</sup> Circumstantial evidence suggests that some of the beneficial effects of RA therapies such as methotrexate<sup>18</sup> and TNF inhibitors<sup>19</sup> may relate to reduced neutrophil recruitment or function. Despite this, there are surprisingly few

studies on the role of neutrophils in the pathogenesis of inflammatory diseases such as RA.

Neutrophil trafficking into tissues is a key step during inflammation, and relies on tightly regulated sequential adhesion events mediated by adhesion molecules expressed by both neutrophils and endothelial cells.<sup>20</sup> Low-affinity interactions involving selectins (E-, P-, and L-selectin) initiate neutrophil rolling along the endothelium. Local chemotactic signals then activate neutrophils to up-regulate cell-surface integrins, which interact with endothelial adhesion molecules resulting in firm adhesion, followed by migration into tissues. In vitro, G-CSF was found to promote adhesion<sup>21-24</sup> and CD11b expression<sup>23,24</sup> by human neutrophils. G-CSF also increased the expression of E-selectin ligands on human myeloid cells.<sup>25</sup> Endothelial cells express G-CSFR<sup>26</sup> and might also respond to G-CSF. Therefore, during inflammatory conditions such as RA, G-CSF may promote inflammation via effects on myeloid cells, endothelial cells, or both. In this study, we investigated potential mechanisms by which G-CSF and neutrophils drive inflammation during CIA.

## Methods

### Mice

Wild-type (WT) C57BL/6 Ly5.2 and Ly5.1 and DBA/1 mice were obtained from the Walter and Eliza Hall Institute (WEHI) Animal Supplies. G-CSF<sup>-/-</sup> mice were kindly provided by Ashley Dunn (Ludwig Institute

Submitted February 22, 2008; accepted September 1, 2008. Prepublished online as *Blood* First Edition paper, September 29, 2008; DOI 10.1182/blood-2008-02-139535.

The online version of this article contains a data supplement.

The publication costs of this article were defrayed in part by page charge payment. Therefore, and solely to indicate this fact, this article is hereby marked "advertisement" in accordance with 18 USC section 1734.

© 2008 by The American Society of Hematology

for Cancer Research, Parkville, Australia),<sup>16</sup> and G-CSFR<sup>-/-</sup> mice were kindly provided by Daniel Link (Washington University Medical School, St Louis, MO).<sup>15</sup> G-CSF<sup>-/-</sup> and G-CSFR<sup>-/-</sup> mice were backcrossed onto the C57BL/6 background for more than 20 and more than 8 generations, respectively. Mice were housed under standard conditions in the WEHI animal facility. All experiments were approved by the institute ethics committee.

## CIA

CIA was induced in C57BL/6 and DBA/1 mice as previously described.<sup>11</sup> On days 0 and 21, mice were injected intradermally at the base of the tail with 0.1 mL of a 1:1 emulsion of chick type II collagen, CII (2 mg/mL in 10 mM acetic acid; Sigma-Aldrich, St Louis, MO) in CFA (5 mg/mL heat-killed *Mycobacterium tuberculosis* strain H37RA [Difco, Detroit, MI] added to incomplete Freund adjuvant [Difco]). This immunization protocol typically causes mild-moderate CIA in C57BL/6 mice and more severe disease in DBA/1 mice. Mice were assessed clinically for swelling and joint restriction, and each paw was scored (0 indicates normal; 1, mild swelling; 2 extensive swelling; and 3, joint distortion and/or rigidity; maximum score per mouse, 12).<sup>11</sup> At the time mice were killed, paws were removed and fixed in 10% (vol/vol) neutral-buffered formalin for at least 2 days. Joints were decalcified for at least 2 days in decalcification buffer (0.4 M HCl, 0.5 M acetic acid, 0.2 M chloroform in 70% [vol/vol] ethanol), which was changed daily. Joints were then embedded in paraffin and frontal sections (5  $\mu$ m) were stained with hematoxylin and eosin (H&E). Histologic assessment of interphalangeal and metacarpophalangeal/metatarsophalangeal joints for arthritis was performed blinded to the experimental groups.

## ELISA for mouse G-CSF

G-CSF levels in sera from naive or CIA mice were measured by capture enzyme-linked immunosorbent assay (ELISA). Immunosorbent plates (NUNC, Roskilde, Denmark) were coated overnight at 4°C with rat antimurine G-CSF mAb (clone 67604; R&D Systems, Minneapolis, MN) in 0.1 M NaHCO<sub>3</sub>, pH 8.2. Plates were kept at room temperature for the remaining procedures and washed with 0.05% (vol/vol) Tween-20 (Sigma Chemical) in PBS between each step. Plates were blocked with 10% (vol/vol) FCS (heat-inactivated; Hyclone, Logan, UT) in PBS for 1 hour, then standards (murine G-CSF; Peprotech, Rocky Hill, NJ) or serum diluted in PBS with 10% (vol/vol) FCS was added for 2 hours. Biotinylated rabbit antimurine G-CSF pAb (Peprotech) in PBS with 10% (vol/vol) FCS were added for 2 hours, followed by streptavidin-horseradish peroxidase (DAKO-Cytomation, Glostrup, Denmark) for 1 hour. Plates were developed with 3,3',5,5'-tetramethylbenzidine (Sigma-Aldrich) substrate (0.1 mg/mL diluted in 0.1 M sodium acetate buffer, pH 8.0, containing 0.003% [vol/vol] H<sub>2</sub>O<sub>2</sub>). The color reaction was stopped with 0.5 M H<sub>2</sub>SO<sub>4</sub> and the OD was measured at 450 nm on a Multiscan Accent microplate reader (Thermo Labsystems, Helsinki, Finland). The concentration of G-CSF in serum was determined by comparing OD readings to the standard curves.

## Bone marrow chimeras

Bone marrow cells (5–7  $\times$  10<sup>6</sup>) from G-CSF<sup>-/-</sup>, G-CSFR<sup>-/-</sup>, or WT Ly5.1 C57BL/6 mice were injected intravenously into lethally irradiated (2  $\times$  5.5 Gy) WT, G-CSF<sup>-/-</sup>, or G-CSFR<sup>-/-</sup> recipient mice to generate (1) [G-CSF<sup>-/-</sup>]  $\rightarrow$  [WT] mice and [WT]  $\rightarrow$  [G-CSF<sup>-/-</sup>] mice, and (2) [G-CSFR<sup>-/-</sup>]  $\rightarrow$  [WT] mice and [WT]  $\rightarrow$  [G-CSFR<sup>-/-</sup>] chimeric mice. Donor-derived reconstitution was determined 6 weeks after transfer by the analysis of Ly5.1/Ly5.2 expression on peripheral blood leukocytes using flow cytometry. Chimeric mice with more than 85% donor-derived reconstitution were used for subsequent experiments.

## Neutrophil depletion/blockade during CIA

DBA/1 mice typically develop uniformly severe CIA using the immunization protocol described, and so this strain was used to evaluate the effect of neutrophil depletion. CIA was induced in WT DBA/1 mice and on the day of clinical disease onset mice were matched for initial disease severity and randomly allocated for treatment with 0.5 mg anti-Gr-1 (Ly6G/C) mAb

(clone RB6.8C5), anti-Ly6G mAb (clone 1A8), or anti-Mac-1 mAb (clone 5C6) or 0.5 mg isotype control mAbs (1:1 mix of rat IgG2a [clone GL117] and rat IgG2b [clone GL121]). For all depletion experiments, antibodies were administered intraperitoneally on days 1, 4, 7, 10, and 12 of disease, and mice were clinically scored daily for 14 days of antibody treatment. After mice were killed, paws were processed and joints were assessed histologically, blinded to treatment groups.

## Specificity of neutrophil-depleting mAbs before and after CIA

WT DBA/1 mice were primed with CII/CFA for CIA on day 0 and then injected intraperitoneally on days 15, 17, and 20 with 0.5 mg mAb (anti-Gr-1, anti-Ly6G, or 1:1 mix of rat IgG2a and rat IgG2b). Peripheral blood was analyzed on day 22. These time points were chosen to cover the period when serum G-CSF levels rise and clinical features of CIA begin to develop (Figure 1A). Peripheral blood was analyzed by flow cytometry for neutrophils (CD11b<sup>+</sup>, Gr-1<sup>high</sup>), monocytes (CD11b<sup>+</sup>, Gr-1<sup>low</sup>), and CD8 T cells (CD3<sup>+</sup>, CD8<sup>+</sup>). Total peripheral blood white blood cell (WBC) counts were quantitated on an Advia 120 machine (Bayer, Pymble NSW, Australia). Cell numbers were calculated by multiplying percentage of cells (from flow cytometry) by the total cell count. The specificity of anti-Ly6G mAb was also evaluated by analysis of blood from mice at day 14 of mAb treatment in CIA (see "Neutrophil depletion/blockade during CIA").

## In vivo effects of administered G-CSF on leukocyte trafficking

Intravital microscopy was used to evaluate the effects of G-CSF on leukocyte trafficking in the microcirculation of the mouse cremaster muscle. Mice were anaesthetized using a cocktail of ketamine (150 mg/kg) and xylazine (10 mg/kg), and the cremaster muscle was exteriorized for intravital microscopy, as previously described.<sup>27</sup> The microcirculation was visualized using an intravital microscope and video camera images were recorded using a videocassette recorder. Leukocyte-endothelial cell interactions were assessed in postcapillary venules (25–40  $\mu$ m in diameter) and parameters measured included the number of rolling, adherent, and emigrated leukocytes. Microvascular leukocyte interactions were recorded 15 minutes after surgical exteriorization. Data were averaged from 2 to 3 postcapillary venules for each mouse, with the final data representing average data from at least 5 to 6 mice per group. To assess the potential local proinflammatory effects of G-CSF, recombinant human G-CSF (which also binds to mouse G-CSFR; filgrastim, Amgen, Thousand Oaks, CA; 15  $\mu$ g/mL in bicarbonate-buffered saline buffer), or saline as a control, was applied directly to the cremaster muscle of naive mice. To assess the potential for systemically administered G-CSF to modify leukocyte-endothelial cell interactions, G-CSF (10  $\mu$ g), or saline vehicle as control, was injected intraperitoneally and the cremaster muscle microvasculature was examined 4 hours later. These doses of G-CSF were based on previous studies showing exacerbation of CIA.<sup>11</sup> Comparable approaches have been used to demonstrate the effects of a range of cytokines on leukocyte trafficking.<sup>28</sup> In experiments to examine the role of Mac-1 in G-CSF-induced adhesion, mice were injected intravenously with anti-Mac-1 mAb (5C6, 100  $\mu$ g) or isotype control mAb, prior to the acute G-CSF superfusion procedure.

To determine whether neutrophils were the predominant leukocyte undergoing adhesion in response to G-CSF, G-CSF-treated cremaster muscles were imaged using intravital confocal microscopy (Leica SP5; Leica-Microsystems, Mannheim, Germany). Using a modification of a previously published approach,<sup>29</sup> mice received a low dose of PE-conjugated anti-Gr-1 mAb (2  $\mu$ g, intravenous injection) to identify Gr-1<sup>high</sup> neutrophils, and individual postcapillary venules were examined using 543 nm (HeNe laser) illumination at rapid scan rates. FITC-dextran (500 kDa) (17  $\mu$ g, intravenous; Molecular Probes, Leiden, The Netherlands) was used to delineate the microvasculature, imaged via 488 nm excitation (argon laser).

## Multiphoton microscopy of synovial microvessels in the knee joint during CIA

To examine the role of endogenous G-CSF in regulating leukocyte-endothelial cell interactions in the synovial microcirculation, CIA was

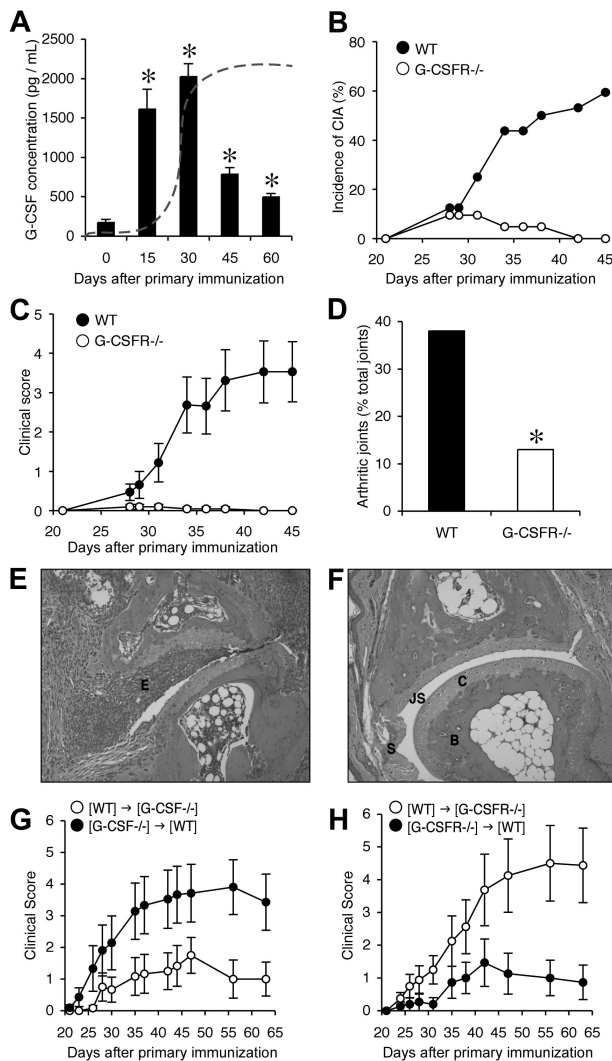


**Figure 1. Critical role for endogenous G-CSF during CIA.** (A) Elevated serum G-CSF levels in WT mice during CIA. Data represent mean plus or minus SEM;  $n > 12$  mice per time point from 2 to 3 independent experiments.  $*P < .001$  compared with naive mice. Dashed line indicates typical profile of clinical features developing in CIA. (B) Reduced incidence of CIA in G-CSFR<sup>-/-</sup> mice. Data represent percentage of total mice.  $P < .001$  at day 45. (C) Reduced clinical scores in G-CSFR<sup>-/-</sup> mice. Data represent mean plus or minus SEM;  $P < .01$  during days 21 to 45.  $n = 21$  to 32 mice per group from 2 independent experiments. (D) Reduced histologic arthritis in joints from G-CSFR<sup>-/-</sup> mice. Data represent percentage of total joints.  $n > 93$  interphalangeal and metacarpophalangeal/metatarsophalangeal joints scored per treatment.  $*P < .005$ . Histologic sections of (E) an arthritic joint from a CIA WT mouse and (F) a typical unaffected joint from a CIA G-CSFR<sup>-/-</sup> mouse. E indicates exudate; JS, joint space; C, cartilage; B, bone; and S, synovium. Magnification,  $\times 100$  (H&E stained). (G) Reduced clinical severity in G-CSF<sup>-/-</sup> mice reconstituted with WT bone marrow ([WT] → [G-CSF<sup>-/-</sup>]) compared with [G-CSF<sup>-/-</sup> → [WT] mice. Data represent mean plus or minus SEM;  $P < .05$  during days 56 to 63.  $n = 12$  to 21 mice per group from 2 independent experiments. (H) Reduced clinical severity in WT mice reconstituted with G-CSFR<sup>-/-</sup> bone marrow ([G-CSFR<sup>-/-</sup> → [WT]) compared with [WT] → [G-CSFR<sup>-/-</sup>] mice.  $P < .05$  during days 21 to 63.  $n = 15$  to 17 mice per group from 2 independent experiments.

induced in WT and G-CSF<sup>-/-</sup> mice. Mice were examined via intravital microscopy 33 to 35 days after the initial immunization for CIA, when WT mice had clinical signs of arthritis. As expected, arthritis was minimal in G-CSF<sup>-/-</sup> mice at this time point. The synovial microcirculation was exposed for intravital microscopy as previously described.<sup>30,31</sup> Neutrophils were stained using PE-conjugated anti-Gr-1 mAb (2  $\mu$ g, intravenous injection), and 500 kDa FITC-dextran (17  $\mu$ g, intravenous injection; Molecular Probes) was used to delineate the microvasculature. Neutrophil rolling and adhesion were assessed in synovial postcapillary venules using a

Leica SP5 multiphoton microscope (Leica-Microsystems) equipped with a 20 $\times$ , 1.0 NA objective and twin nondescanned detectors. Fluorochromes were excited by a MaiTai laser (Spectra Physics, NewSpec, Adelaide, Australia) tuned to 790 nm.

#### Purification of mature neutrophils from mouse bone marrow

Mature neutrophils were purified from bone marrow using a method adapted from Boxio et al.<sup>32</sup> Bone marrow was flushed from the tibiae and femurs of male C57BL/6 WT mice (aged ~8 weeks) into Hanks buffered salt solution (HBSS; GIBCO, Invitrogen, Mount Waverley, Australia) containing 1% (wt/vol) BSA (fraction V; GIBCO, Invitrogen) and 15 mM EDTA. For each neutrophil preparation, bone marrow cells were pooled from at least 2 WT mice and separated using a 3-layered Percoll gradient of 1.110 g/mL, 1.090 g/mL, and 1.083 g/mL Percoll (Amersham, Uppsala, Sweden), with 1 mL per layer in 5-mL polypropylene tubes (BD Falcon, Bedford, MA). Percoll layers were prepared by diluting 100% Percoll (9 parts Percoll + 1 part 10  $\times$  HBSS, pH 7.1) with HBSS. After centrifugation (1500g, 30 minutes, without braking), neutrophils were collected from the 1.110-g/mL to 1.090-g/mL interface. Red blood cells were lysed and neutrophils were washed twice with HBSS (with calcium and magnesium; GIBCO, Invitrogen) containing 1% (wt/vol) BSA. Cells were counted by trypan blue exclusion and purity was assessed by differential counts of cytopsin preparations (10<sup>4</sup> neutrophils per cytopsin) stained with Diff-Quik (Amber Scientific, Midvale, Australia).

#### Flow cytometry analysis of CD62L, LFA-1, and CD11b, and confocal analysis of CD11b

Purified bone marrow neutrophils from WT C57BL/6 mice were stimulated with recombinant human G-CSF (1 pg/mL to 10  $\mu$ g/mL) or saline in the presence or absence of 10  $\mu$ g/mL mouse P-selectin Fc fusion protein (which binds active PSGL-1; BD Pharmingen, San Diego, CA) for 15 or 30 minutes. At each time point, neutrophils were fixed with 4% (wt/vol) paraformaldehyde in PBS for 10 minutes, washed in PBS, incubated with Fc block (clone 2.4G2) for 15 minutes, and stained with PE-conjugated anti-CD62L mAb (clone MEL-14), FITC-conjugated anti-LFA-1 mAb (CD11a/CD18; clone 2D7), or FITC-conjugated anti-CD11b mAb (clone M1/70), for 60 minutes. All incubations were performed at room temperature. A portion of each neutrophil sample was analyzed by flow cytometry and the remaining neutrophils were counterstained with 4',6'-diamidino-2-phenylindole, dihydrochloride (DAPI; diluted 1:1000; Molecular Probes) for 5 minutes. Cytopsin (10<sup>4</sup> neutrophils per cytopsin) were prepared and coverslipped using antifade mounting media (DAKOCytomation). Cytopsin were analyzed using a Leica TCS4 SP2 spectral confocal scanner equipped with 4 lasers and attached to a Leica DMIRE2 motorized inverted microscope (Leica-Microsystems).

#### Statistical analyses

The Student *t* test (2-tailed distribution) was used to analyze serum anti-CII antibody, serum cytokines, T-cell proliferation, cell counts, donor-derived reconstitution in bone marrow chimeras, and systemic G-CSF intravital microscopy data. The permutation statistical test<sup>33</sup> was used to analyze clinical scores over the course of CIA (after boost immunization). The Fisher exact test was used for CIA incidence and the frequency of histologic arthritis. The Student paired *t* test was used to evaluate flow cytometric data of adhesion molecule expression by neutrophils (1-tailed test), and to compare leukocyte trafficking parameters within the same sample group across time for acute G-CSF superfusion experiments (2-tailed test). Two-way ANOVA was used to compare trafficking parameters in G-CSF superfusion experiments using mice pretreated with anti-Mac-1 mAb (5C6) or isotype control. For each test, *P* values less than .05 were considered statistically significant.

## Results

### G-CSF is elevated in the serum of mice with CIA

Serum G-CSF was measured in naive and WT mice that had been immunized for CIA (Figure 1A). G-CSF levels were low but detectable in naive mice (mean  $\pm$  SEM,  $170 \pm 40$  pg/mL). G-CSF levels increased markedly (up to  $2020 \pm 170$  pg/mL by day 30) following initial immunization with type II collagen (CII). Serum G-CSF levels then steadily declined over the following 30 days (day 60,  $500 \pm 40$  pg/mL), but remained significantly elevated compared with naive mice. Importantly, the peak in serum G-CSF corresponded to the early inflammatory phase of CIA and the onset of clinical arthritis (indicated in Figure 1A).

### G-CSFR<sup>-/-</sup> mice are protected against CIA

We previously reported that G-CSF<sup>-/-</sup> mice were markedly protected against CIA.<sup>13</sup> To further dissect the contribution of G-CSF signaling to CIA, we studied mice deficient in the G-CSF receptor (G-CSFR<sup>-/-</sup> mice). Similar to G-CSF<sup>-/-</sup> mice<sup>13</sup> and in sharp contrast to WT mice, G-CSFR<sup>-/-</sup> mice showed few signs of inflammatory arthritis (Figure 1B,C). In G-CSFR<sup>-/-</sup> mice, only 13% of joints showed any histologic evidence of arthritis, and if present this was mild, compared with 38% of joints in WT mice (Figure 1D-F). Inflamed joints from WT mice were extensively infiltrated by inflammatory cells, and showed regions of bone and cartilage destruction (Figure 1E). In contrast, almost all joints from CIA G-CSFR<sup>-/-</sup> mice resembled the typical joints of naive mice (Figure 1F). CII-specific T-cell responses were normal, but anti-CII IgG levels were reduced in G-CSFR<sup>-/-</sup> mice (mean relative units  $\pm$  SEM,  $1.69 \pm 0.45$  in G-CSFR<sup>-/-</sup> mice and  $4.35 \pm 0.8$  in WT mice), consistent with findings in G-CSF<sup>-/-</sup> mice.<sup>13</sup>

### CIA requires nonhematopoietic cell-derived G-CSF and hematopoietic cell-restricted expression of G-CSFR

Preliminary studies showed that G-CSF injections in G-CSF<sup>-/-</sup> mice immunized for CIA restored disease (data not shown), demonstrating there are no developmental abnormalities in G-CSF<sup>-/-</sup> mice that might prevent the generation of CIA. G-CSFR is expressed by leukocytes<sup>34</sup> and endothelial cells,<sup>26</sup> and a variety of cells can produce G-CSF.<sup>14,35</sup> To identify sources of G-CSF production and responses during the disease process of CIA, reciprocal bone marrow chimeras were generated using G-CSF<sup>-/-</sup>, G-CSFR<sup>-/-</sup>, and WT mice. CIA was reduced in G-CSF-deficient recipients of WT bone marrow cells ([WT]  $\rightarrow$  [G-CSF<sup>-/-</sup>] mice, day-63 mean clinical score  $\pm$  SEM,  $1.0 \pm 0.5$ ) compared with [G-CSF<sup>-/-</sup>]  $\rightarrow$  [WT] mice ( $3.4 \pm 0.9$ ; Figure 1G), demonstrating that nonhematopoietic cells are the major producers of G-CSF during CIA. There was reduced CIA in [G-CSFR<sup>-/-</sup>]  $\rightarrow$  [WT] mice (day-63 clinical score, mean  $\pm$  SEM,  $0.9 \pm 0.5$ ) compared with [WT]  $\rightarrow$  [G-CSFR<sup>-/-</sup>] mice ( $4.4 \pm 1.1$ , Figure 1H), demonstrating that hematopoietic cells are the primary targets of G-CSF during CIA. Although the clinical severity in each "protected" chimera pair was greater than G-CSF<sup>-/-</sup> or G-CSFR<sup>-/-</sup> mice, this most likely reflects the potentially confounding effect of less than 100% donor-derived reconstitution (mean  $\pm$  SEM,  $91.2\% \pm 0.5\%$ ). Of note, in each chimera pair, reduced CIA was associated with relative neutropenia prior to immunization ([WT]  $\rightarrow$  [G-CSF<sup>-/-</sup>] mice, mean percentage of neutrophils/WBC  $\pm$  SEM,  $3.5 \pm 0.7$  vs  $15.6 \pm 1.2$  in [G-CSF<sup>-/-</sup>]  $\rightarrow$  [WT]; and [G-CSFR<sup>-/-</sup>]  $\rightarrow$  [WT] mice,  $5.6 \pm 0.8$  vs  $18.9 \pm 1.1$  in [WT]  $\rightarrow$  [G-CSFR<sup>-/-</sup>]).

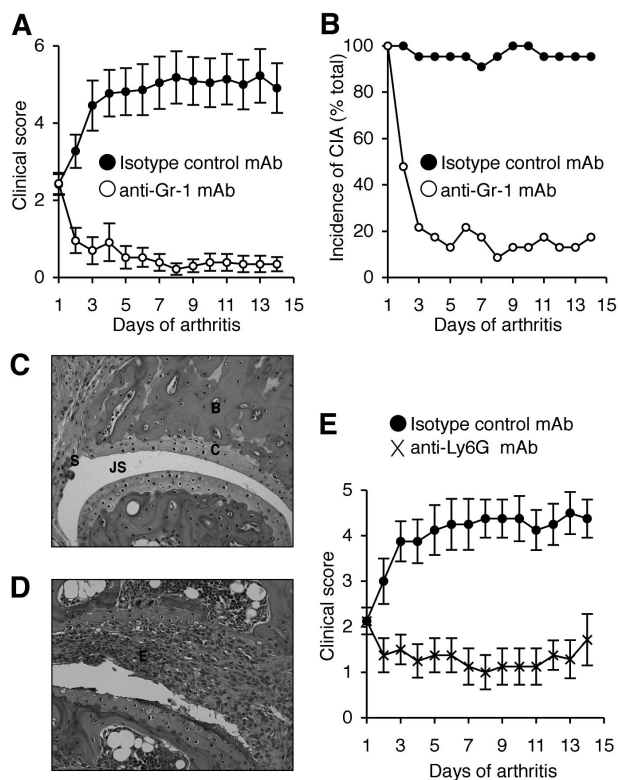


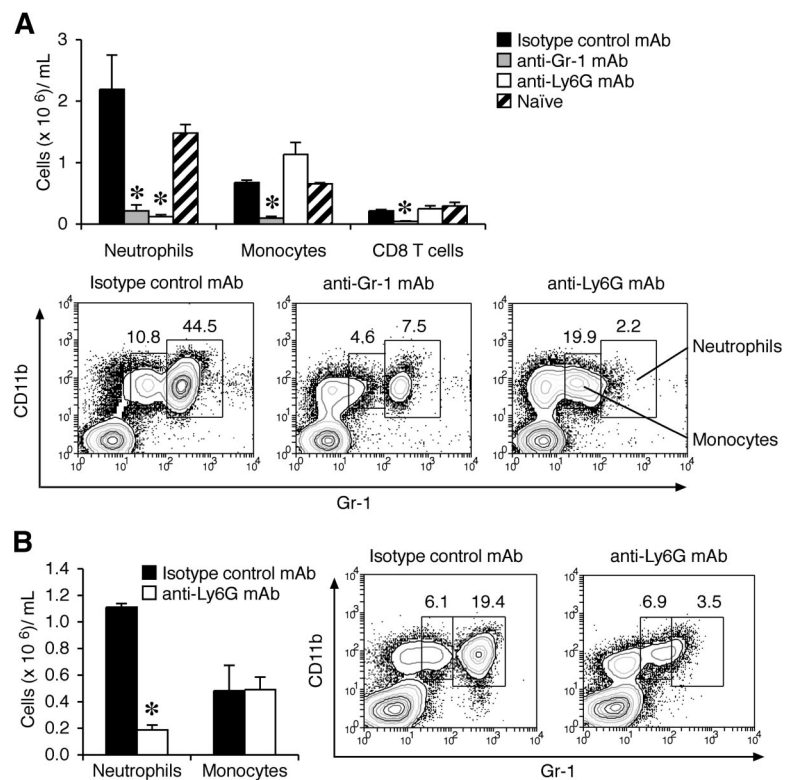
**Figure 2. Neutrophil depletion attenuates established CIA.** (A) Clinical scores (mean  $\pm$  SEM) in WT DBA/1 mice treated with either isotype control mAb or anti-Gr-1 mAb after the onset of CIA.  $P < .001$  during days 1 to 14 of arthritis. (B) Incidence of disease (percentage of total mice) in isotype control and anti-Gr-1 mAb-treated mice during 14 days of treatment.  $P < .001$  at day 14. In panels A and B,  $n = 22$  to 23 mice per treatment group; data pooled from 3 independent experiments. Histologic sections of typical joints from (C) anti-Gr-1 mAb and (D) isotype control mAb-treated mice. E indicates exudate; JS, joint space; C, cartilage; B, bone; and S, synovium. Magnification,  $\times 200$  (H&E stained). (E) Clinical scores (mean  $\pm$  SEM) in WT DBA/1 mice treated with either isotype control mAb or anti-Ly6G mAb (1A8) after the onset of CIA.  $n = 8$  mice per treatment group.  $P < .01$  during days 1 to 14 of arthritis.

### Reduced CIA in neutrophil-depleted mice

We previously showed that neutralization of G-CSF after the onset of CIA reduced disease progression.<sup>13</sup> To directly assess the role of neutrophils in CIA, anti-Gr-1 mAb (clone RB6.8C5) was used to deplete neutrophils in DBA/1 mice (the most CIA-responsive strain) after the clinical onset of disease. On day 1 of disease, treatment groups were matched for disease severity (mean  $\pm$  SEM,  $2.4 \pm 0.3$ ). Disease progressed in isotype control mAb-treated mice, resulting in a 2-fold increase in clinical severity by day 14 ( $4.9 \pm 0.6$ ; Figure 2A) and the incidence of CIA was maintained (Figure 2B). In contrast, the severity of CIA in mice treated with anti-Gr-1 mAb actually declined over the course of antibody treatment (day 14,  $0.4 \pm 0.2$ ; Figure 2A) and only 4 of 23 mice showed any clinical signs of disease by day 14 (Figure 2B). The beneficial effect of anti-Gr-1 mAb treatment appeared rapidly, and most mice showed reduced clinical features of CIA within 2 days of commencing treatment. Histologic assessment revealed that only 35% of joints in anti-Gr-1 mAb-treated mice were arthritic (usually mild), compared with 75% of joints in isotype control mAb-treated mice ( $P < .001$ ). Representative sections are shown (Figure 2C,D).

Gr-1 (Ly6C/G) is also expressed at lower levels on subsets of monocytes, CD8<sup>+</sup> T cells, and plasmacytoid dendritic cells.<sup>36-38</sup> Although anti-Gr-1 has been widely used in the literature for neutrophil depletion studies, anti-Ly6G mAb (1A8) is reported to

**Figure 3. Effects of anti-Gr-1 (Ly6G/C) and anti-Ly6G mAbs on depletion of neutrophils before and after the onset of CIA.** (A) Myeloid and CD8 T-cell counts in peripheral blood (cells  $\times 10^6$ /mL blood; mean  $\pm$  SEM) from mice with high G-CSF levels (day 22 after CII/CFA immunization). WT DBA/1 mice were primed with CII/CFA, then injected intraperitoneally on days 15, 17, and 20 with 0.5 mg mAb (anti-Gr-1, anti-Ly6G, or 1:1 mix of rat IgG2a and rat IgG2b) and analyzed on day 22 ( $n = 4$  mice per treatment). \* $P < .05$ . (B) Myeloid cell counts in WT DBA/1 mice treated with either isotype control mAb or anti-Ly6G mAb 14 days after the onset of CIA. \* $P < .001$ . Representative flow cytometric profiles are shown in panels A and B. Numbers indicate the percentage of total cells within the gate.



be more specific.<sup>39</sup> It is also possible that the depleting effects of these antibodies differ once G-CSF levels are high, so we also evaluated this question in mice primed for CIA. Under these conditions, anti-Ly6G mAb specifically depleted neutrophils (Figure 3A,B), whereas anti-Gr-1 mAb also depleted monocytes and CD8 T cells (Figure 3A). Of note, plasmacytoid dendritic cells do not express Ly6G and are not depleted by 1A8 mAb.<sup>37</sup> To validate our finding that neutrophils are critical for disease progression during CIA, mice with established arthritis were treated with anti-Ly6G mAb. Similar to anti-Gr-1 mAb depletion, anti-Ly6G mAb treatment after the onset of CIA blocked disease progression in WT DBA/1 mice (Figure 2E).

### G-CSF promotes leukocyte trafficking in vivo

G-CSF has been shown to promote neutrophil adhesion in vitro,<sup>21-24</sup> and both leukocytes<sup>34</sup> and endothelial cells<sup>26</sup> express G-CSFR. In our previous experiments,<sup>13</sup> G-CSF blockade after the onset of CIA had a rapid therapeutic effect, raising the possibility of effects downstream of neutrophil production. To assess whether G-CSF promotes leukocyte recruitment in vivo, the microvasculature of the cremaster muscle was visualized with intravital microscopy. We first examined the acute effect of locally administered G-CSF. There was no significant difference in rolling flux between saline- and G-CSF-treated groups at time 0 ( $P = .11$ ,  $n = 6-8$  mice/treatment group). G-CSF reduced rolling flux at 30 minutes (Figure 4A), and rapidly increased leukocyte adhesion in postcapillary venules, which was evident within 15 minutes and persisted at 30 minutes (Figure 4B). This response was comparable with that induced by a suboptimal concentration of the chemotactic agent KC, which induced adhesion of approximately 10 cells and emigration of 9 to 10 cells (data not shown). In comparison, G-CSF exposure over 45 minutes led to approximately 7 cells adhering and emigrating. In vivo confocal microscopy using PE-conjugated anti-Gr-1 mAb identified all adherent cells in

G-CSF-treated muscle as Gr-1<sup>+</sup> neutrophils (Figure 4C; Video S1). There was minimal adhesion of Gr-1<sup>+</sup> cells in saline-treated mice, and G-CSF induced adhesion of a similar number of total leukocytes as observed with conventional intravital microscopy (data not shown).

Previous studies showed that G-CSF can increase CD11b expression on human neutrophils.<sup>23,24</sup> Mice were therefore pretreated with anti-Mac-1 (CD18/CD11b) blocking mAb, 5C6, via intravenous injection and then G-CSF was administered locally to assess whether G-CSF-induced leukocyte trafficking in vivo was Mac-1 dependent. Anti-Mac-1 pretreatment had no effect on rolling flux (Figure 4D). In contrast, G-CSF-induced adhesion was abolished in mice pretreated with anti-Mac-1 (Figure 4E). In these experiments, assessment of the G-CSF-induced response out to 45 minutes revealed that local G-CSF administration also induced leukocyte transmigration (Figure 4F). This was also significantly reduced in 5C6-pretreated mice. Mac-1 is therefore critical for the enhanced leukocyte trafficking induced by G-CSF.

Intravital microscopy was used to also examine effects of systemic G-CSF on leukocyte trafficking in vivo. In contrast to the acute effect of G-CSF on leukocyte rolling, 4-hour systemic treatment with G-CSF did not alter leukocyte rolling flux (Figure 5A). However, leukocyte adhesion and emigration were significantly increased in postcapillary venules 4 hours after intraperitoneal injection of G-CSF (Figure 5A). Prolonged exposure to G-CSF may increase leukocyte trafficking via effects on leukocytes or endothelial cells, or both. To assess the relative contribution of these cell types, 4-hour G-CSF responses were tested in mice rendered chimeric for the G-CSFR. It has been previously observed that the leukocyte trafficking response to inflammatory mediators can be altered by the processes of bone marrow transplantation via irradiation and reconstitution.<sup>40</sup> It was therefore necessary to establish that following irradiation and bone marrow reconstitution, G-CSF (4-hour) treatment retained the ability to induce a

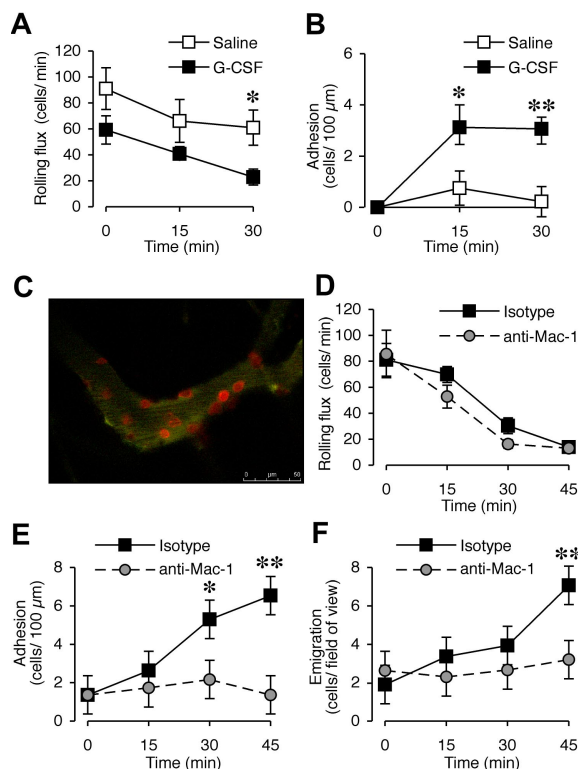


**Figure 4. Acute local administration of G-CSF promotes Mac-1-dependent adhesion and transendothelial migration of neutrophils in vivo.** (A) Leukocyte rolling flux and (B) adhesion in postcapillary venules (vessel diameter 25–40  $\mu\text{m}$ ) of cremaster muscle before and after superfusion with saline or 15  $\mu\text{g}/\text{mL}$  G-CSF for up to 30 minutes in WT C57BL/6 mice.  $n = 6$  to 8 mice per group.  $*P < .05$ ;  $**P < .001$  versus basal adhesion, or versus saline rolling flux. (C) In vivo confocal image using PE-conjugated anti-Gr-1 mAb showing that adherent cells in G-CSF-treated muscle are Gr-1<sup>+</sup> neutrophils. (D) Leukocyte rolling flux, (E) adhesion, and (F) transendothelial migration in postcapillary venules of cremaster muscle before and after superfusion with 15  $\mu\text{g}/\text{mL}$  G-CSF for up to 45 minutes in WT C57BL/6 mice that were pretreated (intravenous injection) with anti-Mac-1 mAb (5C6) or isotype control mAb.  $n = 5$  mice per group. Data represent mean plus or minus SEM;  $*P < .05$ ;  $**P < .001$ .

leukocyte response. Importantly, G-CSF responses in [WT]  $\rightarrow$  [WT] mice (Figure 5B) were comparable with those in WT mice (Figure 5A), indicating that the process of generating chimeric mice had not altered the G-CSF response. However, the scale of the response was somewhat reduced relative to nonirradiated mice, consistent with previous studies.<sup>40</sup> The G-CSF response in [WT]  $\rightarrow$  [G-CSFR<sup>-/-</sup>] mice was equivalent to that in [WT]  $\rightarrow$  [WT] mice (Figure 5C), whereas G-CSF failed to induce leukocyte rolling, adhesion, or emigration in mice lacking expression of G-CSFR on hematopoietic cells ([G-CSFR<sup>-/-</sup>]  $\rightarrow$  [WT] mice; Figure 5C). This finding demonstrates that systemic G-CSF acts directly upon leukocytes to promote transendothelial migration into tissues, independent of any G-CSF-induced endothelial cell response.

#### G-CSF decreases CD62L expression and increases CD11b expression by neutrophils

Adhesion molecules expressed by both leukocytes and endothelial cells regulate leukocyte trafficking into tissues. Constitutive expression of P-selectin and ICAM-1 by vascular endothelial cells within the cremaster muscle is sufficient to support some leukocyte rolling and adhesion, respectively.<sup>28,41</sup> Interestingly, G-CSF induced a reduction in CD62L (L-selectin) expression by neutrophils in vitro (Figure 6A). This is consistent with our finding that acute G-CSF

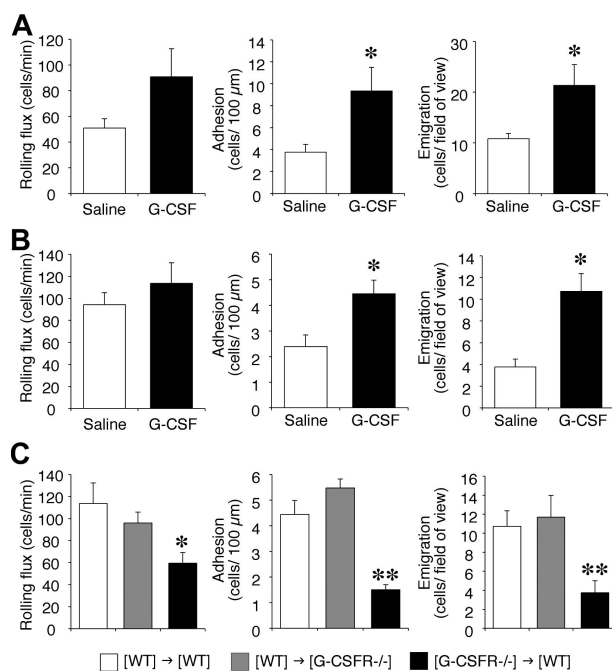


**Figure 5. Systemic administration of G-CSF promotes leukocyte trafficking in vivo and this response depends on G-CSFR expression by leukocytes.** (A) Leukocyte trafficking in postcapillary venules of cremaster muscle in WT C57BL/6 mice 4 hours after intraperitoneal injection with saline or 10  $\mu\text{g}$  G-CSF.  $n = 6$  mice per group.  $*P < .05$ . (B) Leukocyte trafficking in postcapillary venules of cremaster muscle in WT mice reconstituted with WT bone marrow cells ([WT]  $\rightarrow$  [WT]) 4 hours after intraperitoneal injection with saline or 10  $\mu\text{g}$  G-CSF.  $n = 6$  mice per group.  $*P < .01$ . (C) Leukocyte trafficking in postcapillary venules of cremaster muscle in bone marrow chimeric mice 4 hours after intraperitoneal injection with 10  $\mu\text{g}$  G-CSF showing normal responses in G-CSFR<sup>-/-</sup> mice reconstituted with WT bone marrow cells ([WT]  $\rightarrow$  [G-CSFR<sup>-/-</sup>]), but impaired G-CSF-induced leukocyte trafficking in WT mice reconstituted with G-CSFR<sup>-/-</sup> bone marrow cells ([G-CSFR<sup>-/-</sup>]  $\rightarrow$  [WT]).  $n = 6$  mice per group.  $*P < .05$ ;  $**P < .005$ . Shown in panels A to C from left to right; leukocyte rolling flux, adhesion, and transendothelial migration. Data represent mean plus or minus SEM.

administration reduced rolling flux in vivo. In vitro stimulation with G-CSF had little effect on LFA-1 expression by neutrophils (Figure 6B). In contrast, G-CSF rapidly increased surface expression of CD11b on neutrophils in vitro (Figure 6C). Previously, it was shown that ligation of neutrophil PSGL-1 to P-selectin activated  $\beta 2$ -integrin-mediated adhesion of mouse and human neutrophils.<sup>42,43</sup> Given the rapid neutrophil adhesion response induced by G-CSF in vivo, and the well-recognized ability of stimulated leukocytes to up-regulate adhesion molecules, we examined whether G-CSF in combination with P-selectin fusion protein (which binds to active PSGL-1) increased surface expression of CD11b. Interestingly, the combination of G-CSF and P-selectin fusion protein further increased CD11b expression (Figure 6C), suggesting that G-CSF may potentiate the adhesion of neutrophil rolling on P-selectin. Representative confocal microscopy images after 30-minute treatment are shown (Figure 6D-F).

#### Reduced adhesion of neutrophils in synovial microvessels of G-CSF<sup>-/-</sup> mice during CIA

The synovium is the major site of tissue inflammation in CIA and so multiphoton microscopy was used to examine the interactions of Gr-1<sup>+</sup> cells in synovial microvessels. Synovial tissue from the knee joints of WT and G-CSF<sup>-/-</sup> mice was examined when clinical disease was apparent in WT mice (days 33–35). Exposure of the knee joint at this time point in WT mice revealed a neutrophil-rich

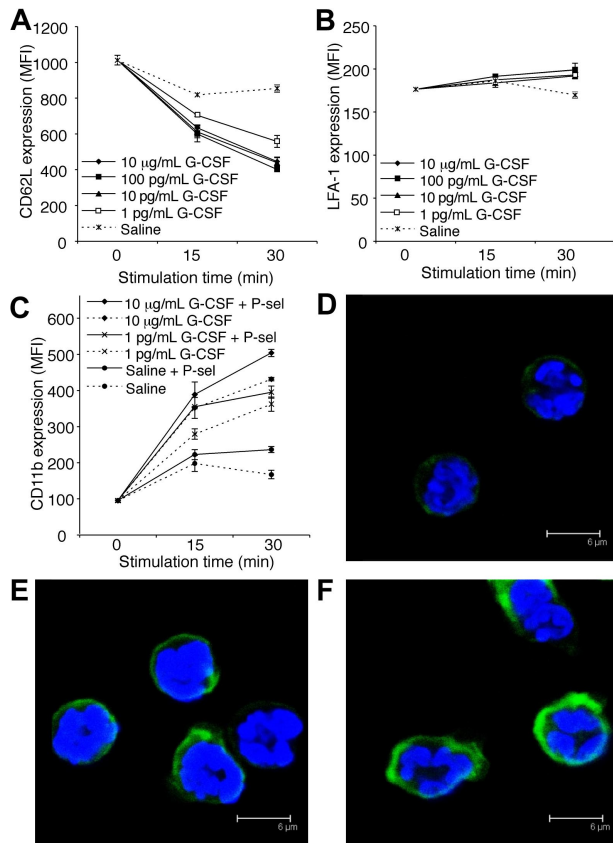


**Figure 6. G-CSF decreases CD62L and increases CD11b expression by neutrophils in vitro.** (A) CD62L expression on purified neutrophils treated in vitro with G-CSF (1 pg/mL–10  $\mu$ g/mL) or saline.  $P < .05$ ; at 15 and 30 minutes, saline versus 1 to 100 pg/mL or 10  $\mu$ g/mL G-CSF. (B) LFA-1 (CD11a/CD18) expression on purified neutrophils treated in vitro with G-CSF (1 pg/mL–10  $\mu$ g/mL) or saline.  $P < .05$ ; saline versus 100 pg/mL G-CSF at 15 minutes, saline versus 1 to 100 pg/mL or 10  $\mu$ g/mL G-CSF at 30 minutes. (C) CD11b expression on purified neutrophils treated with or without G-CSF, in the presence or absence of P-selectin fusion protein (P-sel; 10  $\mu$ g/mL).  $P < .05$  at 15 and 30 minutes; saline versus 1 to 100 pg/mL or 10  $\mu$ g/mL G-CSF, each dose of G-CSF alone versus the equivalent dose of G-CSF + P-selectin. Data in panels A to C show mean MFI (mean fluorescence intensity) plus or minus SD for duplicate samples, representative of at least 2 independent experiments, each using neutrophils pooled from 4 WT C57BL/6 mice. Representative confocal images showing CD11b in green and DAPI-stained nuclei in blue of neutrophils treated for 30 minutes with (D) saline, (E) 10  $\mu$ g/mL G-CSF, or (F) 10  $\mu$ g/mL G-CSF and 10  $\mu$ g/mL P-selectin fusion protein (P-sel).

exudate. In contrast, very little exudate was visible in the knee joints of G-CSF<sup>-/-</sup> mice (data not shown). Rolling flux within the synovial microvessels was comparable in WT and G-CSF<sup>-/-</sup> mice (Figure 7A). In WT mice, adhesion of Gr-1<sup>+</sup> leukocytes (neutrophils) was more than 6 cells/100  $\mu$ m, well above our previously published levels of basal leukocyte adhesion in this vascular bed,<sup>30</sup> indicating a robust adhesion response (Figure 7B,C). In contrast, neutrophil adhesion in synovial microvessels of G-CSF<sup>-/-</sup> mice was rare, and significantly lower than that in WT mice (Figure 7B,D).

#### Disease progression in CIA depends on Mac-1–mediated leukocyte trafficking

In view of our intravital and multiphoton microscopy findings, Mac-1 was blocked after the onset of CIA using the mAb 5C6. Similar to neutrophil depletion, Mac-1 blockade effectively prevented disease progression in mice with established CIA (Figure 7E). This result demonstrates that progression of CIA requires Mac-1–mediated trafficking of leukocytes.

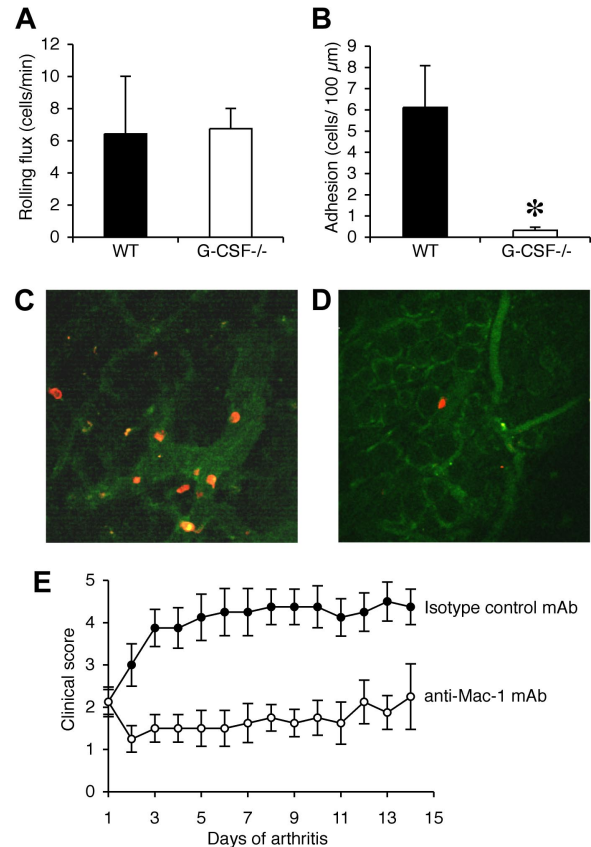


**Figure 7. Neutrophil adhesion in synovial microvessels is reduced in G-CSF<sup>-/-</sup> mice during CIA and leukocyte trafficking during CIA is Mac-1 dependent.** (A) Rolling flux (cells/min) and (B) adhesion (number of adherent cells/100  $\mu$ m) within the synovial microvessels of WT and G-CSF<sup>-/-</sup> mice with CIA. \* $P < .05$ . Representative multiphoton microscopy images of adherent Gr-1<sup>+</sup> cells (red/orange) in synovial microvessels in the knee joint synovium of (C) WT and (D) G-CSF<sup>-/-</sup> mice when clinical evidence of CIA was apparent in WT mice (days 33–35). (E) Clinical scores (mean  $\pm$  SEM) in mice treated with either isotype control mAb or Mac-1 blocking mAb (5C6) after the onset of CIA.  $n = 8$  mice per treatment group. The effect of 5C6 on the progression of CIA was compared with an isotype control mAb-treated group of mice within the 1 experiment, as shown here and in Figure 2E.  $P < .01$  during days 1 to 14 of arthritis.

## Discussion

Human and animal studies<sup>2,3,5,10–13</sup> suggest that G-CSF has an important role during inflammatory arthritis. In the current study, we sought to understand how G-CSF deficiency produces such marked protection against CIA, which is the most widely used murine model of RA. We found that serum G-CSF is elevated during CIA, correlating with the onset of clinical features. Similar to G-CSF<sup>-/-</sup> mice,<sup>13</sup> G-CSFR<sup>-/-</sup> mice were largely protected against CIA. We therefore generated bone marrow chimeras and showed that during CIA, nonhematopoietic cells are the major source of G-CSF production. Potential nonhematopoietic sources of G-CSF in CIA require further evaluation, but include bone marrow stromal cells, synovial fibroblasts, chondrocytes and endothelial cells.<sup>14,35</sup> What triggers these cells to make G-CSF during CIA is an important but unresolved question, and may involve inflammatory cytokines including IL-17 and IL-23.<sup>44</sup> The bone marrow chimera results also clearly demonstrate that although G-CSFR is expressed by a variety of nonhematopoietic cells including endothelial cells, hematopoietic cells are the major

responders to G-CSF during CIA. Reduced CIA was also associated with relative neutropenia and so, collectively, these results focused our further studies onto the effects of G-CSF on mature neutrophils. To directly assess the requirement for neutrophils during CIA, neutrophils were depleted once CIA was clinically established, using either anti-Gr-1 (Ly6G/C) mAb (clone RB6.8C5) or anti-Ly6G mAb (clone 1A8). Even after disease onset, neutrophil depletion with both of these antibodies arrested the progression of CIA, demonstrating a critical requirement for these cells in perpetuating joint inflammation.

To explore proinflammatory effects of G-CSF on neutrophils, we used intravital microscopy to directly examine whether G-CSF can promote leukocyte trafficking in vivo. To our knowledge, these are the first intravital microscopy studies on G-CSF. Locally administered G-CSF rapidly increased leukocyte adhesion and transendothelial migration, and the adherent leukocytes were identified as neutrophils. This response was Mac-1 dependent, and G-CSF increased Mac-1 expression on neutrophils, demonstrating that Mac-1 activation is the dominant mechanism for this in vivo trafficking response. The combination of G-CSF and PSGL-1 ligation further increased CD11b expression on neutrophils, suggesting that, in vivo, G-CSF may enhance the adhesion of neutrophils that are already rolling on endothelial P-selectin. Although acute, local G-CSF administration increased neutrophil adhesion and transmigration, it attenuated leukocyte rolling. Consistent with this finding, G-CSF down-regulated the expression of CD62L (L-selectin) expression by neutrophils in vitro. Furthermore, G-CSF is reported to rapidly down-regulate PSGL-1 expression on human neutrophils,<sup>45</sup> which may also explain the effect we observed on neutrophil rolling.

Having established that local G-CSF can regulate Mac-1-dependent neutrophil adhesion in the short term, we also analyzed the adhesion response to systemic G-CSF over a longer period (4 hours). Leukocyte adhesion and transmigration were also enhanced by G-CSF under these conditions. Bone marrow chimeras confirmed that this prolonged response also relies on G-CSFR expression by leukocytes, rather than endothelial cells. However, in contrast to acute, local G-CSF administration, leukocyte rolling was not reduced in response to 4-hour G-CSF stimulation, unless hematopoietic cells lacked G-CSFR. These observations suggest that the reduction in rolling induced by acute, local G-CSF administration may be opposed by a different response to extended G-CSF exposure. In support of this contention, we have observed that exposure of neutrophils to G-CSF for 4-hour in vitro induced up-regulation of PSGL-1 mRNA (J.L.E., S.F.D., unpublished observations, 2006), which could act to maintain leukocyte rolling. Sustained exposure to G-CSF therefore has the potential to change cellular responses relative to acute G-CSF exposure, via induction of gene transcription in neutrophils.

Multiphoton confocal microscopy was used to directly examine neutrophil trafficking in the synovium, which is the major site of tissue inflammation in CIA. Adhesion of Gr-1<sup>+</sup> neutrophils to blood vessels in synovial tissue of the knee was clearly increased in WT mice with CIA and, consistent with our intravital microscopy findings in muscle tissue, there was a significant reduction in neutrophil adhesion within the synovial blood vessels of G-CSF<sup>-/-</sup> mice. In contrast, there was no major difference in rolling of Gr-1<sup>+</sup> neutrophils in synovial blood vessels between WT mice with CIA and G-CSF<sup>-/-</sup> mice. These data are consistent with our intravital microscopy findings in muscle tissue following prolonged systemic exposure to G-CSF and provide direct evidence that endogenous G-CSF enhances neutrophil trafficking in the synovium during

CIA. The importance of Mac-1-dependent leukocyte trafficking in CIA was evaluated in vivo. Consistent with our in vitro observations, administration of anti-Mac-1 mAb blocked disease progression in mice with established CIA.

Collectively, our studies provide further evidence that G-CSF is a critical mediator of inflammatory arthritis, and identify neutrophils as key effector cells that promote the progression of disease. We have previously demonstrated that immune activation during CIA results in G-CSF-driven hematopoiesis, and using bone marrow chimeras we now show that these events are mediated by cells outside of the hematopoietic compartment. We also show that G-CSF can directly regulate neutrophil trafficking in vivo, which may explain why G-CSF blockade produced a rapid effect even after the onset of CIA.<sup>13</sup> It may also be relevant to understanding the vascular and inflammatory complications observed in some patients after treatment with G-CSF.<sup>1-9</sup> Our studies highlight the potential for G-CSF to initiate and amplify inflammatory responses and provide a strong rationale for therapeutic modulation of G-CSF during autoimmune arthritis, and potentially in other conditions where neutrophils exacerbate sterile tissue inflammation.

## Acknowledgments

We thank A. Dunn (Ludwig Institute for Cancer Research) for G-CSF<sup>-/-</sup> mice and D. Link (Washington University Medical School) for G-CSFR<sup>-/-</sup> mice; Rain Kwan (Center for Inflammatory Diseases, Monash University) for intravital microscopy assistance; M. Leech (Center for Inflammatory Diseases, Monash University) for assistance with the synovial microcirculation preparation; A. van Nieuwenhuijze (WEHI) for flow cytometry assistance; J. Corbin (WEHI) for Advia cell counts; S. Mihajlovic and staff (WEHI) for histology; and J. Merryfull, K. Brown, and J. Stewart (WEHI) for animal husbandry.

This work was supported by the Reid Charitable Trusts (Melbourne, Australia), the National Health and Medical Research Council (Canberra, Australia; project grant 461243, program grant 461219, practitioner fellowships 215408 [I.P.W.] and 356213 [A.W.R.]; industry fellowship 461287 [I.K.C.]).

## Authorship

Contribution: J.L.E. and M.J.H. performed research, analyzed and interpreted data, performed statistical analysis, and wrote the paper; M.U.N. and W.G.J. performed research, analyzed and interpreted data, and performed statistical analysis; B.A.C. performed research and analyzed data; A.W.R. designed research, interpreted data, and wrote the paper; S.F.D. performed research and analyzed data; D.M. designed and performed research and wrote the paper; I.K.C. designed and performed research and analyzed and interpreted data; and I.P.W. designed research, analyzed and interpreted data, and wrote the paper.

Conflict-of-interest disclosure: I.P.W. has acted as a scientific consultant to Murigen and CSL on the development of G-CSF antagonists. The remaining authors declare no competing financial interests.

Correspondence: Ian P. Wicks, Reid Rheumatology Laboratory, Division of Autoimmunity and Transplantation, The Walter and Eliza Hall Institute of Medical Research, 1G Royal Parade, Parkville, Victoria 3050, Australia; e-mail: wicks@wehi.edu.au.



## References

- Lindemann A, Rumberger B. Vascular complications in patients treated with granulocyte colony-stimulating factor (G-CSF). *Eur J Cancer*. 1993; 29A:2338-2339.
- Schots R, Verbruggen LA, Demanet C. G-CSF in Felty's syndrome: correction of neutropenia and effects on cytokine release. *Clin Rheumatol*. 1995;14:116-118.
- Stricker RB, Goldberg B. G-CSF and exacerbation of rheumatoid arthritis. *Am J Med*. 1996;100:665-666.
- Fukumoto Y, Miyamoto T, Okamura T, et al. Angina pectoris occurring during granulocyte colony-stimulating factor-combined preparatory regimen for autologous peripheral blood stem cell transplantation in a patient with acute myelogenous leukaemia. *Br J Haematol*. 1997;97:666-668.
- Snowden JA, Biggs JC, Milliken ST, et al. A randomized, blinded, placebo-controlled, dose escalation study of the tolerability and efficacy of filgrastim for haemopoietic stem cell mobilisation in patients with severe active rheumatoid arthritis. *Bone Marrow Transplant*. 1998;22:1035-1041.
- Adler BK, Salzman DE, Carabasi MH, Vaughan WP, Reddy VV, Prchal JT. Fatal sickle cell crisis after granulocyte colony-stimulating factor administration. *Blood*. 2001;97:3313-3314.
- Dereure O, Hillaire-Buys D, Guilhou JJ. Neutrophil-dependent cutaneous side-effects of leucocyte colony-stimulating factors: manifestations of a neutrophil recovery syndrome? *Br J Dermatol*. 2004;150:1228-1230.
- Hill JM, Syed MA, Arai AE, et al. Outcomes and risks of granulocyte colony-stimulating factor in patients with coronary artery disease. *J Am Coll Cardiol*. 2005;46:1643-1648.
- Arimura K, Inoue H, Kukita T, et al. Acute lung injury in a healthy donor during mobilization of peripheral blood stem cells using granulocyte-colony stimulating factor alone. *Haematologica*. 2005;90:ECR10.
- Nakamura H, Ueki Y, Sakito S, et al. High serum and synovial fluid granulocyte colony stimulating factor (G-CSF) concentrations in patients with rheumatoid arthritis. *Clin Exp Rheumatol*. 2000; 18:713-718.
- Campbell IK, Rich MJ, Bischof RJ, Hamilton JA. The colony-stimulating factors and collagen-induced arthritis: exacerbation of disease by M-CSF and G-CSF and requirement for endogenous M-CSF. *J Leukoc Biol*. 2000;68:144-150.
- Miyahara H, Hotokebuchi T, Saikawa I, Arita C, Takagishi K, Sugioka Y. The effects of recombinant human granulocyte colony-stimulating factor on passive collagen-induced arthritis transferred with anti-type II collagen antibody. *Clin Immunol Immunopathol*. 1993;69:69-76.
- Lawlor KE, Campbell IK, Metcalf D, et al. Critical role for granulocyte colony-stimulating factor in inflammatory arthritis. *Proc Natl Acad Sci U S A*. 2004;101:11398-11403.
- Roberts AW. G-CSF: a key regulator of neutrophil production, but that's not all! *Growth Factors*. 2005;23:33-41.
- Liu F, Wu HY, Wesselschmidt R, Kornaga T, Link DC. Impaired production and increased apoptosis of neutrophils in granulocyte colony-stimulating factor receptor-deficient mice. *Immunity*. 1996;5:491-501.
- Lieschke GJ, Grail D, Hodgson G, et al. Mice lacking granulocyte colony-stimulating factor have chronic neutropenia, granulocyte and macrophage progenitor cell deficiency, and impaired neutrophil mobilization. *Blood*. 1994;84:1737-1746.
- Pillinger MH, Abramson SB. The neutrophil in rheumatoid arthritis. *Rheum Dis Clin North Am*. 1995;21:691-714.
- Kraan M, de Koster B, Elferink J, Post W, Breedveld F, Tak P. Inhibition of neutrophil migration soon after initiation of treatment with leflunomide or methotrexate in patients with rheumatoid arthritis: findings in a prospective, randomized, double-blind clinical trial in fifteen patients. *Arthritis Rheum*. 2000;43:1488-1495.
- Paleolog EM, Hunt M, Elliott MJ, Feldmann M, Maini RN, Woody JN. Deactivation of vascular endothelium by monoclonal anti-tumor necrosis factor alpha antibody in rheumatoid arthritis. *Arthritis Rheum*. 1996;39:1082-1091.
- Luster AD, Alon R, von Andrian UH. Immune cell migration in inflammation: present and future therapeutic targets. *Nat Immunol*. 2005;6:1182-1190.
- Chakraborty A, Hentzen ER, Seo SM, Smith CW. Granulocyte colony-stimulating factor promotes adhesion of neutrophils. *Am J Physiol Cell Physiol*. 2003;284:C103-C110.
- Okada Y, Kawagishi M, Kusaka M. Effect of recombinant human granulocyte colony-stimulating factor on human neutrophil adherence in vitro. *Experientia*. 1990;46:1050-1053.
- Yong KL, Linch DC. Differential effects of granulocyte- and granulocyte-macrophage colony-stimulating factors (G- and GM-CSF) on neutrophil adhesion in vitro and in vivo. *Eur J Haematol*. 1992; 49:251-259.
- Yuo A, Kitagawa S, Ohsaka A, et al. Recombinant human granulocyte colony-stimulating factor as an activator of human granulocytes: potentiation of responses triggered by receptor-mediated agonists and stimulation of C3b1 receptor expression and adherence. *Blood*. 1989;74:2144-2149.
- Dagia NM, Gadhoum SZ, Knoblauch CA, et al. G-CSF induces E-selectin ligand expression on human myeloid cells. *Nat Med*. 2006;12:1185-1190.
- Bocchietto E, Guglielmetti A, Silvagno F, et al. Proliferative and migratory responses of murine microvascular endothelial cells to granulocyte-colony-stimulating factor. *J Cell Physiol*. 1993; 155:89-95.
- Norman MU, Lister KJ, Yang YH, Issekutz A, Hickey MJ. TNF regulates leukocyte-endothelial cell interactions and microvascular dysfunction during immune complex-mediated inflammation. *Br J Pharmacol*. 2005;144:265-274.
- Gregory JL, Morand EF, McKeown SJ, et al. Macrophage migration inhibitory factor induces macrophage recruitment via CC chemokine ligand 2. *J Immunol*. 2006;177:8072-8079.
- Chiang EY, Hidalgo A, Chang J, Frenette PS. Imaging receptor microdomains on leukocyte subsets in live mice. *Nat Methods*. 2007;4:219-222.
- Gregory JL, Leech MT, David JR, Yang YH, Dacumos A, Hickey MJ. Reduced leukocyte-endothelial cell interactions in the inflamed microcirculation of macrophage migration inhibitory factor-deficient mice. *Arthritis Rheum*. 2004;50:3023-3034.
- Veihelmann A, Szczesny G, Nolte D, Krombach F, Refior HJ, Messmer K. A novel model for the study of synovial microcirculation in the mouse knee joint in vivo. *Res Exp Med (Berl)*. 1998;198:43-54.
- Boxio R, Bossenmeyer-Pourie C, Steinckwich N, Dournon C, Nusse O. Mouse bone marrow contains large numbers of functionally competent neutrophils. *J Leukoc Biol*. 2004;75:604-611.
- Elso CM, Roberts LJ, Smyth GK, et al. Leishmaniasis host response loci (Imr1-3) modify disease severity through a Th1/Th2-independent pathway. *Genes Immun*. 2004;5:93-100.
- Nicola NA, Metcalf D. Binding of 125I-labeled granulocyte colony-stimulating factor to normal murine hemopoietic cells. *J Cell Physiol*. 1985; 124:313-321.
- Campbell IK, Novak U, Cebon J, Layton JE, Hamilton JA. Human articular cartilage and chondrocytes produce hemopoietic colony-stimulating factors in culture in response to IL-1. *J Immunol*. 1991;147:1238-1246.
- Geissmann F, Jung S, Littman DR. Blood monocytes consist of two principal subsets with distinct migratory properties. *Immunity*. 2003;19:71-82.
- Asselin-Paturel C, Brizard G, Pin JJ, Briere F, Trinchieri G. Mouse strain differences in plasmacytoid dendritic cell frequency and function revealed by a novel monoclonal antibody. *J Immunol*. 2003;171:6466-6477.
- Matsuzaki J, Tsuji T, Chamoto K, Takeshima T, Sendo F, Nishimura T. Successful elimination of memory-type CD8+ T cell subsets by the administration of anti-Gr-1 monoclonal antibody in vivo. *Cell Immunol*. 2003;224:98-105.
- Daley JM, Thomay AA, Connolly MD, Reichner JS, Albina JE. Use of Ly6G-specific monoclonal antibody to deplete neutrophils in mice. *J Leukoc Biol*. 2008;83:64-70.
- Mazo IB, Quackenbush EJ, Lowe JB, von Andrian UH. Total body irradiation causes profound changes in endothelial traffic molecules for hematopoietic progenitor cell recruitment to bone marrow. *Blood*. 2002; 99:4182-4191.
- Jung U, Ley K. Regulation of E-selectin, P-selectin, and intercellular adhesion molecule 1 expression in mouse cremaster muscle vasculature. *Microcirculation*. 1997;4:311-319.
- Blanks JE, Moll T, Eytner R, Vestweber D. Stimulation of P-selectin glycoprotein ligand-1 on mouse neutrophils activates beta 2-integrin mediated cell attachment to ICAM-1. *Eur J Immunol*. 1998;28:433-443.
- Ma YQ, Plow EF, Geng JG. P-selectin binding to P-selectin glycoprotein ligand-1 induces an intermediate state of alphaMbeta2 activation and acts cooperatively with extracellular stimuli to support maximal adhesion of human neutrophils. *Blood*. 2004;104:2549-2556.
- Stark MA, Huo Y, Burcin TL, Morris MA, Olson TS, Ley K. Phagocytosis of apoptotic neutrophils regulates granulopoiesis via IL-23 and IL-17. *Immunity*. 2005;22:285-294.
- Jilma B, Hergovich N, Homoncik M, Marsik C, Kreuzer C, Jilma-Stohlawetz P. Rapid down modulation of P-selectin glycoprotein ligand-1 (PSGL-1, CD162) by G-CSF in humans. *Transfusion*. 2002;42:328-333.